J Solid State Electrochem (2007) 11: 93–102
DOI 10.1007/s10008-005-0076-9

ORIGINAL PAPER

San Ping Jiang

Activation, microstructure, and polarization of solid oxide fuel cell cathodes

Received: 18 July 2005 / Revised: 17 September 2005 / Accepted: 3 October 2005 / Published online: 29 November 2005

Abstract Activation effect can be defined as the enhancement of the electrochemical performance or activity of the solid oxide fuel cell cathodes such as Sr-doped $LaMnO_3$ (LSM) with the polarization/current passage treatment under fuel cell operation conditions. In this paper, the activation effect of the cathodic polarization/current passage on the O_2 reduction reaction of the LSM-based cathodes is reviewed. In addition to the activation effect, cathodic polarization/current passage also has a significant effect on the microstructure of the LSM electrodes and the morphology between the LSM electrode and Y_2O_3-ZrO_2 electrolyte interface. A mechanism involving the incorporation of SrO species into the LSM lattice and the formation of oxygen vacancies is proposed for the activation effect of the polarization.

Keywords Activation · Cathodic polarization · Fuel cells · Microstructure · Sr-doped $LaMnO_3$ · Review

Introduction

It is well known that for the O_2 reduction reaction on the cathode of solid oxide fuel cells such as Sr-doped $LaMnO_3$ (LSM), the electrode performance improves significantly after the application of a cathodic polarization or a cathodic current passage [1–3]. The improvement in the electrode performance is characterized by the rapid decrease in the cathodic polarization potential and/or the electrode polarization (interface) resistance (R_E) after the cathodic polarization or current passage treatment. The reduction in the cathodic polarization potential is due to the reduction in the overpotentials for the O_2 reduction reaction as the change in the electrode ohmic resistance is generally negligible. This significant enhancement of the electrochemical activity with the cathodic polarization/current treatment is also reported for the LSM/Y_2O_3-ZrO_2 (YSZ) composite cathodes [4–6] and metallic electrodes such as Pt [7, 8]. Such nonstationary or activation process is not new and has been known to the fuel cell communities for a long time, as reviewed briefly by McEvoy [9]. Clearly, the activation process is a very important phenomenon and is of great practical relevance as the electrode performance not only depends on the fabrication process (i.e., the microstructure), but also on the testing history. Unfortunately, little is known on the mechanism of the activation process under cathodic polarization, and the activation phenomena are poorly documented. In the case of Pt electrodes, the activation process of the electrode is due to the decomposition of Pt-O surface species under cathodic polarization/current passage because of the existence of the PtO_x surface species on the metal surface [7, 10]. For the O_2 reduction on LSM cathodes, the situation is much more complex. Early researchers attributed the activation behavior to the formation of oxygen vacancies in LSM at high cathodic polarization, which could significantly increase the oxygen diffusion process by opening a parallel transport pathway through the LSM bulk [11–15]. However, it has been observed experimentally that the relaxation time of the electrode performance is typically in the scale of several hours even at temperatures of 700–900°C rather than minutes as would be expected from the relatively fast anion diffusion [11]. The hysteresis of the LSM cathode for the O_2 reduction reaction is shown to be inductive, i.e., the hysteresis becomes wider with decreasing scan rate [12]. If the oxygen vacancy formation is the only mechanism for the activation effect, one would expect this hysteresis to close with decreasing scan rate. This indicates that the oxygen vacancy formation under polarization cannot be the only explanation.

In this paper, the effect of the polarization on the performance enhancement, microstructure, and electrode/electrolyte interface in the system of Sr-doped $LaMnO_3$ electrode and YSZ electrolyte is reviewed. Polarization/current treatment has a significant effect not only on the activation and enhancement of the electrochemical activity

S. P. Jiang (✉)
School of Mechanical and Aerospace Engineering,
Nanyang Technological University,
50 Nanyang Ave.,
639798 Singapore, Singapore
e-mail: mspjiang@ntu.edu.sg
Fax: +65-67911892

of the electrode, but also on the microstructure and interface morphology between LSM electrode and YSZ electrolyte. The origin of the activation effect of the cathodic polarization/current passage treatment is discussed, and a hypothesis is proposed that the activation process of the LSM electrode is associated with the incorporation of oxide species such as the SrO species that is originally segregated on the LSM surface and with the removal of cation vacancies, followed by the formation of oxygen vacancies under the influence of cathodic polarization.

The effect of cathodic polarization on the performance

The best example for the activation phenomena is the initial polarization and impedance behavior of a freshly prepared LSM electrode with the cathodic polarization/current passage treatment. Figure 1 shows the typical polarization behavior of an A-site deficient $La_{0.72}Sr_{0.18}MnO_3$ for the O_2 reduction and impedance responses measured at open circuit [16]. For the O_2 reduction reaction on the freshly prepared LSM electrodes, the initial polarization losses are very high and decrease significantly with the cathodic polarization/current passage. Consistent with the polarization potential, the impedance responses at zero DC bias decrease rapidly with the application of the cathodic current passage. For example, the initial electrode polarization resistance, R_E, is 6.2 Ω cm^2, and after cathodic current treatment for 15 min, R_E is reduced to 0.7 Ω cm^2 (Fig. 1b). The reduction in the electrode polarization resistance is substantial. The analysis of the impedance responses as a function of the cathodic current passage indicates that the effect of the cathodic polarization is primarily on the reduction in the low-frequency impedance [2]. As shown by McEvoy [9], the considerable elapsed time at a fixed temperature of 840°C or a temperature excursion to 900°C has little effect on the impedance responses for the reaction on a lanthanum-deficient LSM. The impedance responses only decrease significantly after the passing of a current of ~300 mA cm^{-2} for 20 min. The enhanced polarization behavior was maintained at 840°C for at least 24 h. This indicates that the activation process under the cathodic polarization/current passage is also not a simple transient phenomenon.

Leng et al. [6] observed the activation effect of cathodic polarization/current passage on the polarization and impedance behavior of LSM (50 wt.%)/YSZ (50 wt.%) composite electrodes. Figure 2 shows the initial impedance responses of an A-site stoichiometry $(La_{0.85}Sr_{0.15})_{1.0}MnO_3$/YSZ (LSM-A/YSZ) and an A-site nonstoichiometry $(La_{0.85}Sr_{0.15})_{0.9}MnO_3$/YSZ (LSM-B/YSZ) composite cath-

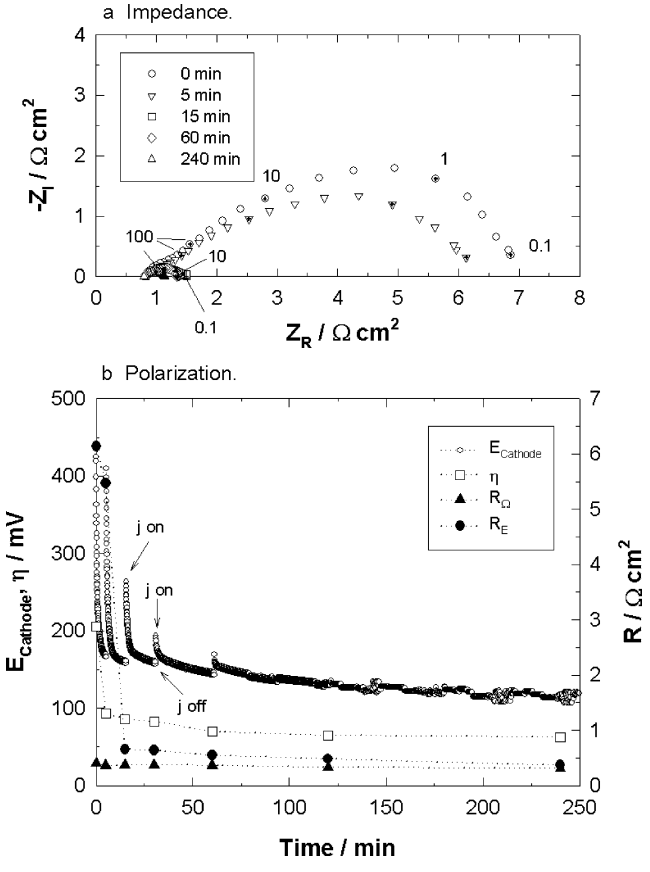

Fig. 1 **a** Impedance and **b** polarization behavior of a freshly prepared $La_{0.72}Sr_{0.18}MnO_3$ electrode for the O_2 reduction reaction as a function of cathodic polarization time at 200 mA cm^{-2} and 900°C in air. The impedance responses were measured at open circuit, and the *numbers* are the frequencies in hertz [16]

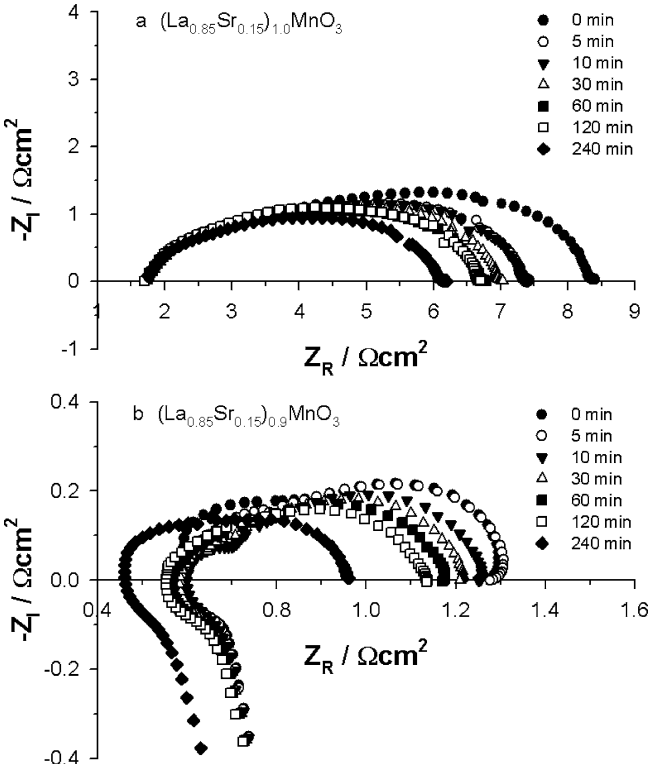

Fig. 2 Initial impedance responses of **a** an A-site stoichiometry $(La_{0.85}Sr_{0.15})_{1.0}MnO_3$/YSZ and **b** an A-site nonstoichiometry $(La_{0.85}Sr_{0.15})_{0.9}MnO_3$/YSZ composite cathode as a function of cathodic current passage time at 200 mA cm^{-2} and 800°C in air. The impedance responses were measured at open circuit [6]

odes as a function of cathodic current passage time at 200 mA cm^{-2} and 800°C in air. The impedance responses were measured at open circuit. The size of the impedance arc decreases with the cathodic current passage time, indicating the activation effect of the cathodic polarization on the electrochemical activity of the LSM/YSZ composite cathodes. However, the electrode interface resistance and the activation effect of the cathodic current treatment for the O_2 reduction on the A-site nonstoichiometry LSM-B/YSZ composite cathode are significantly smaller in magnitude as compared to that of the A-site stoichiometry LSM-A/YSZ composite cathode. For example, for the LSM-A/YSZ cathode, R_E decreased from 8.3 to 5.5 Ω cm^2 after the passing cathodic polarization/current of 200 mA cm^{-2} for 240 min. In the case of LSM-B/YSZ composite cathode, it decreased from an initial value of 0.72 to 0.5 Ω cm^2 under the same cathodic current treatment conditions. The much higher electrode interface resistance for the reaction on LSM-A/YSZ composite cathode is probably due to the formation of a resistive phase between LSM-A and YSZ [2, 17]. The effect of the LSM composition on the activation process of the LSM/YSZ composite is also reported by others. Lee et al. [18] studied the effect of cathodic current passage on the impedance behavior of stoichiometry $La_{1-x}Sr_xMnO_3$/YSZ (50/50) composite cathodes with x=0, 0.1, 0.15, 0.2, 0.3, 0.4, and 0.5 and observed that the effect of the cathodic polarization varied with the LSM composition. After passing a cathodic current of 1 A cm^{-2} for 24 h at 900°C, the impedance responses that were measured 4 min after switching off the cathodic current decreased for cells with x=0, 0.1, and 0.2. However, the impedance measured 24 h after switching off the current showed a significant increase in the electrode interface resistance for all cells, with the exception of the $La_{0.8}Sr_{0.2}MnO_3$/YSZ composite cathode. No explanations are given for the observed behavior. McIntosh et al. [4] also reported a significant activation effect of polarization on the performance of $(La_{0.85}Sr_{0.15})_{1.0}MnO_3$/YSZ composite cathodes. The electrode interface resistance of the cathode decreased significantly after passing a cathodic current of 100 mA cm^{-2} for 10 min at 700°C, starting from a value of more than 12 Ω cm^2 and decreasing to less than 5 Ω cm^2. A similar activation effect of the cathodic polarization on the LSM/YSZ composite cathodes is also reported by Kim et al. [5]. Nevertheless, the activation effect of the cathodic polarization/current passage on LSM/YSZ composite cathodes appears to be much smaller than that on pure LSM electrodes (see Fig. 1).

In contrast to the activation effect of the cathodic polarization, the anodic polarization would be expected to have a deactivation effect on the polarization performance of the LSM cathode. Figure 3 shows the electrode polarization resistance (R_E) of the freshly prepared LSM electrodes under various polarization treatment programs at 200 mA cm^{-2} and 800°C [19]. For the O_2 reduction on a freshly prepared LSM electrode, the electrode polarization resistance decreased rapidly with the cathodic polarization

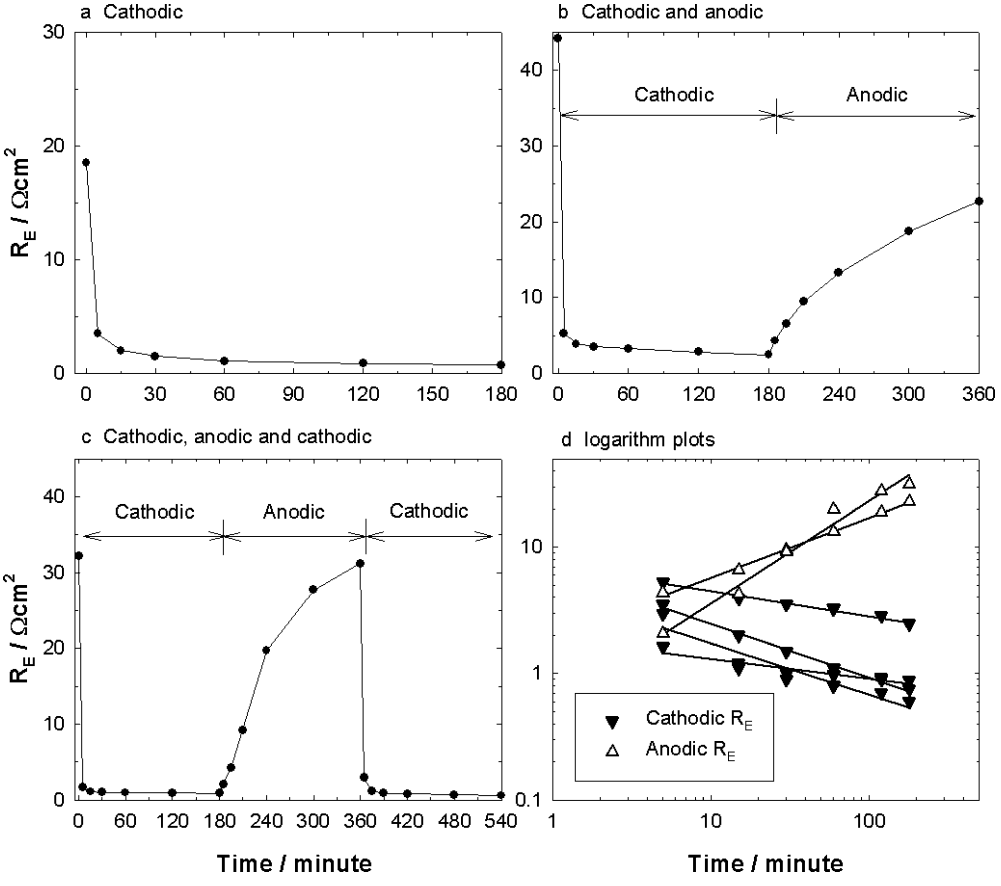

Fig. 3 Electrode polarization resistance (R_E) of freshly prepared LSM electrodes under various polarization treatment programs at 200 mA cm^{-2} and 800°C after [19] **a** cathodic polarization for 3 h; **b** cathodic and anodic polarization for 6 h; **c** cathodic, anodic, and cathodic polarization for 9 h; and **d** logarithm plot of R_E

treatment (Fig. 3a). On the other hand, R_E increased monotonically with subsequent anodic current passage, and the rate of increase in R_E with the anodic polarization treatment was much slower than the corresponding decrease rate of R_E with the cathodic polarization treatment (Fig. 3b). The increase in R_E is an indication of the deactivation effect of the anodic polarization on the O_2 reaction at LSM electrodes. Similar to the observations made on the freshly prepared LSM electrode, R_E decreased very rapidly with a further subsequent cathodic current passage. However, the initial decrease in the R_E appears not to be as sharp as that observed on the freshly prepared LSM electrodes (Fig. 3c). The order of the decrease in the electrode polarization resistance with respect to the polarization time is −0.30±0.12 in average (i.e., $R_E \propto t^{-0.30\pm0.12}$), while the order of the increase in the electrode polarization resistance is +0.64±0.17 (i.e., $R_E \propto t^{+0.64\pm0.17}$, see Fig. 3d). This indicates that the deactivation of the anodic polarization/current treatment and the activation process of the cathodic polarization/current treatment for the reaction on LSM electrodes may not exactly be reversible.

Effect of polarization on microstructure and microstructural stability

The change in the microstructure under the influence of the polarization has been reported on LSM-based cathodes by various research groups. Tsukuda and Yamashita [20] observed the microstructure change at the LSM/YSZ interface region after the cathodic current passage treatment. In the study of the impedance responses of the $La_{0.8}Sr_{0.2}MnO_3$ cathode/YSZ electrolyte interface, Kuznecov et al. [21] observed the formation of nanopores near the cathode/electrolyte interface after the aging of the LSM cathode at a DC voltage of 0.8 V for 3 h (Fig. 4). We have systematically investigated the effect of the polarization on the microstructure and the morphology of the LSM electrode [19, 22]. Both cathodic and anodic polarization/current treatments have an influence on the microstructure change of the LSM electrode/electrolyte interface region and in the electrode bulk itself. The microstructure of a freshly prepared LSM electrode is characterized by large agglomerates with no clear boundaries between LSM grains. After various polarization treatments (e.g., cathodic, anodic, or combined polarization), large agglomerates disappear, and the microstructure of the LSM electrode is characterized by much smaller and well-defined granular-shaped particles with clear boundaries. The morphology change caused by the cathodic current passage treatment cannot be reversed by a subsequent anodic current passage treatment. Such a microstructural change occurs on the electrode surface as well as at the electrode/electrolyte interface. This indicates that the microstructure change under polarization is not due to the local heating as suggested by Tsukuda and Yamashita [20]. The microstructural change under polarization was also observed for the A-site stoichiometry composition LSM [3].

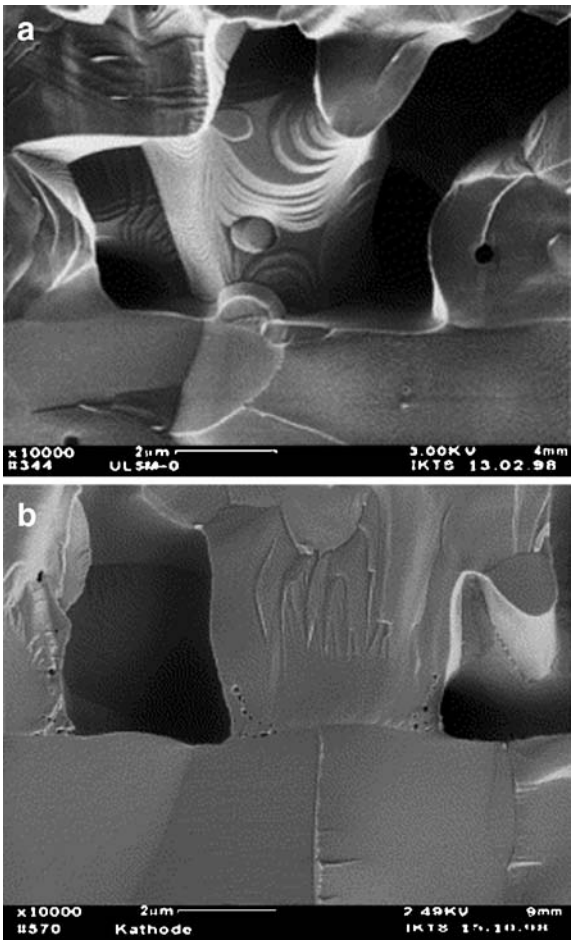

Fig. 4 Formation of nanopores near the cathode/electrolyte interface. **a** Initial state and **b** after the aging of the LSM cathode at a DC voltage of 0.8 V for 3 h [21]

The cathodic polarization also has a significant effect on the microstructural stability of LSM cathodes under solid oxide fuel cell (SOFC) operation conditions in comparison to that at open circuit under the same temperatures [23]. Figure 5 shows the scanning electron microscope (SEM) images of the $(La_{0.8}Sr_{0.2})_xMnO_3$ (x=1.0, 0.9, 0.8) electrode tested with and without a current load of 500 mA cm^{-2} at 1,000°C in air for 1,600 h. In all cases, a coarsening of the LSM particles can be observed regardless of the current load in comparison with the initial grain size. For example, the initial grain size of the $(La_{0.8}Sr_{0.2})_{0.9}MnO_3$ electrode before the test was 0.78±0.286 μm. After sintering at 1,000°C under a current load of 500 mA cm^{-2} for 1,600 h, the grain size of the LSM electrode was 0.88±0.302 μm. In the case of the LSM electrode sintered at open circuit under the same conditions, the LSM grains grew to 1.174±0.251 μm, which is 33% larger than that sintered under current load. The grains of the LSM electrodes sintered under cathodic polarization are in fact smaller than that sintered without current load. The same trend is observed for the LSM electrodes with different stoichiometrical compositions, as shown in Fig. 6. The grain size measurements from the SEM analysis revealed a higher grain growth of the LSM electrodes sintered at open circuit

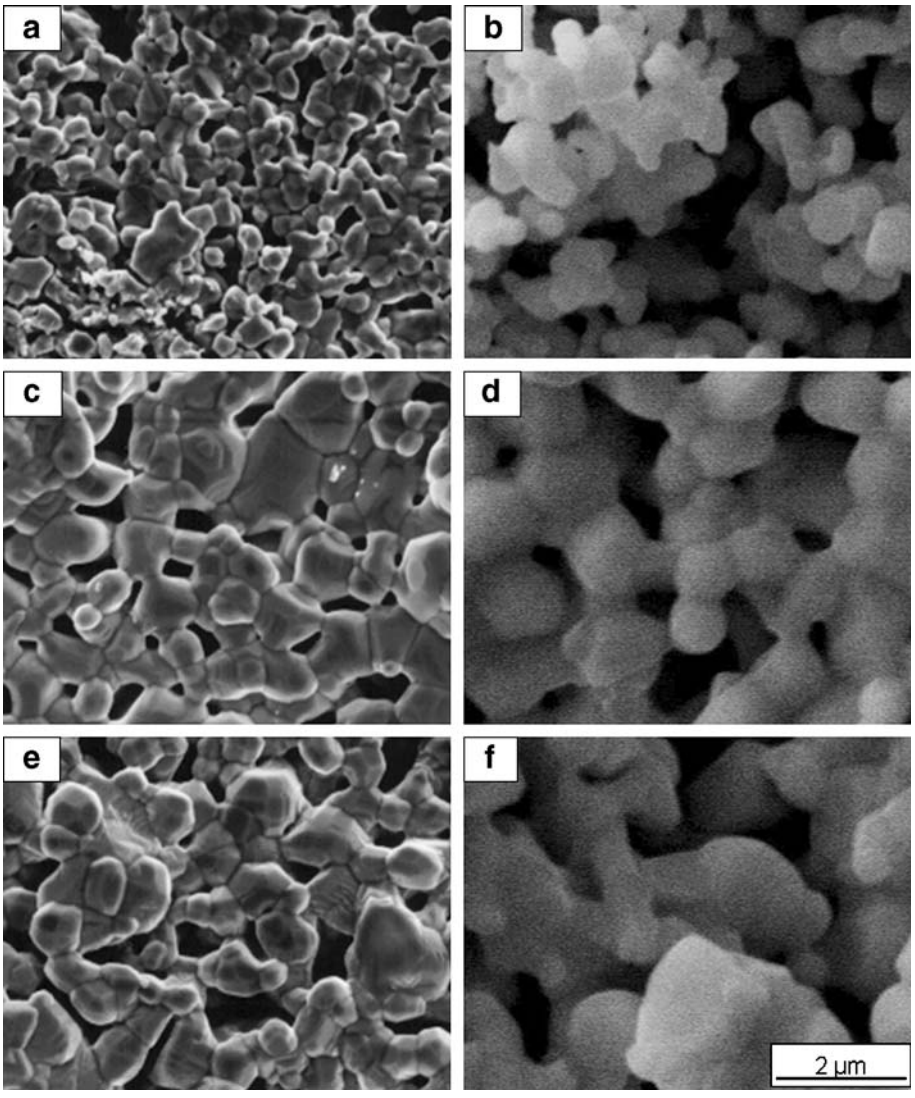

Fig. 5 SEM micrographs of the $(La_{0.8}Sr_{0.2})_xMnO_3$ electrode surface of **a** x=1.0, **c** x=0.9, and **e** x=0.8 tested under a current load of 500 mA cm^{-2} and **b** x=1.0, **d** x=0.9, and **f** x=0.8 tested without a current load at 1,000°C in air for 1,600 h. Scale bar applies to all SEM micrographs [23]

in comparison to that sintered under cathodic polarization conditions at 1,000°C. The reduced sintering under cathodic polarization could be related to the elimination of the cation vacancies at the A−sites, thus reducing the driving force for the sintering and grain growth of the LSM electrodes [23].

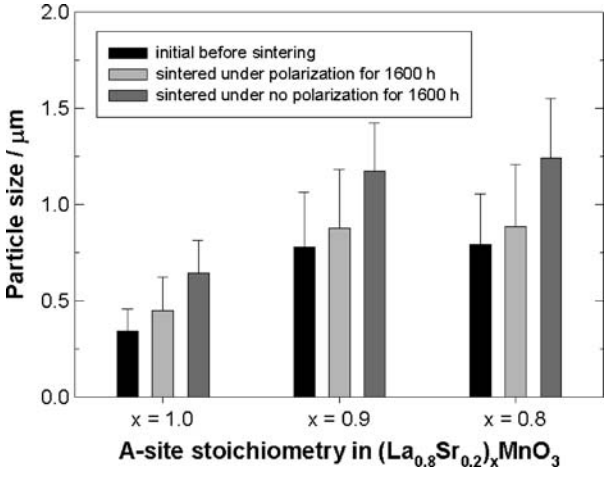

Fig. 6 Plots of the particle size of LSM electrodes sintered at 1,000°C in air with and without a current load of 500 mA cm^{-2} for 1,600 h as a function of A-site stoichiometry composition [23]

Polarization not only influences the microstructure change of the LSM electrode but also causes a morphological change at the interface between the LSM cathode and YSZ electrolyte. An atomic force microscopy (AFM) study of the YSZ electrolyte surface in contact with the LSM electrode before and after various polarization treatments clearly shows the interfacial change, as shown in Fig. 7 [24]. After removing the LSM electrode coating by HCl acid treatment, rings or dents approximately 0.5–1.0 μm in diameter can clearly be seen on the YSZ surface (Fig. 7a). They grew out of the YSZ electrolyte, forming convex-shaped rings on the YSZ surface. The rings have sharp boundaries and a depth in the range of 90 to 140 nm. The location of these rings on the YSZ surface shows a random distribution, either on the smooth surface of YSZ grains or at the grain boundaries. This indicates that the rings are the contact points between LSM particles and the YSZ surface. No square islands were formed on the convex

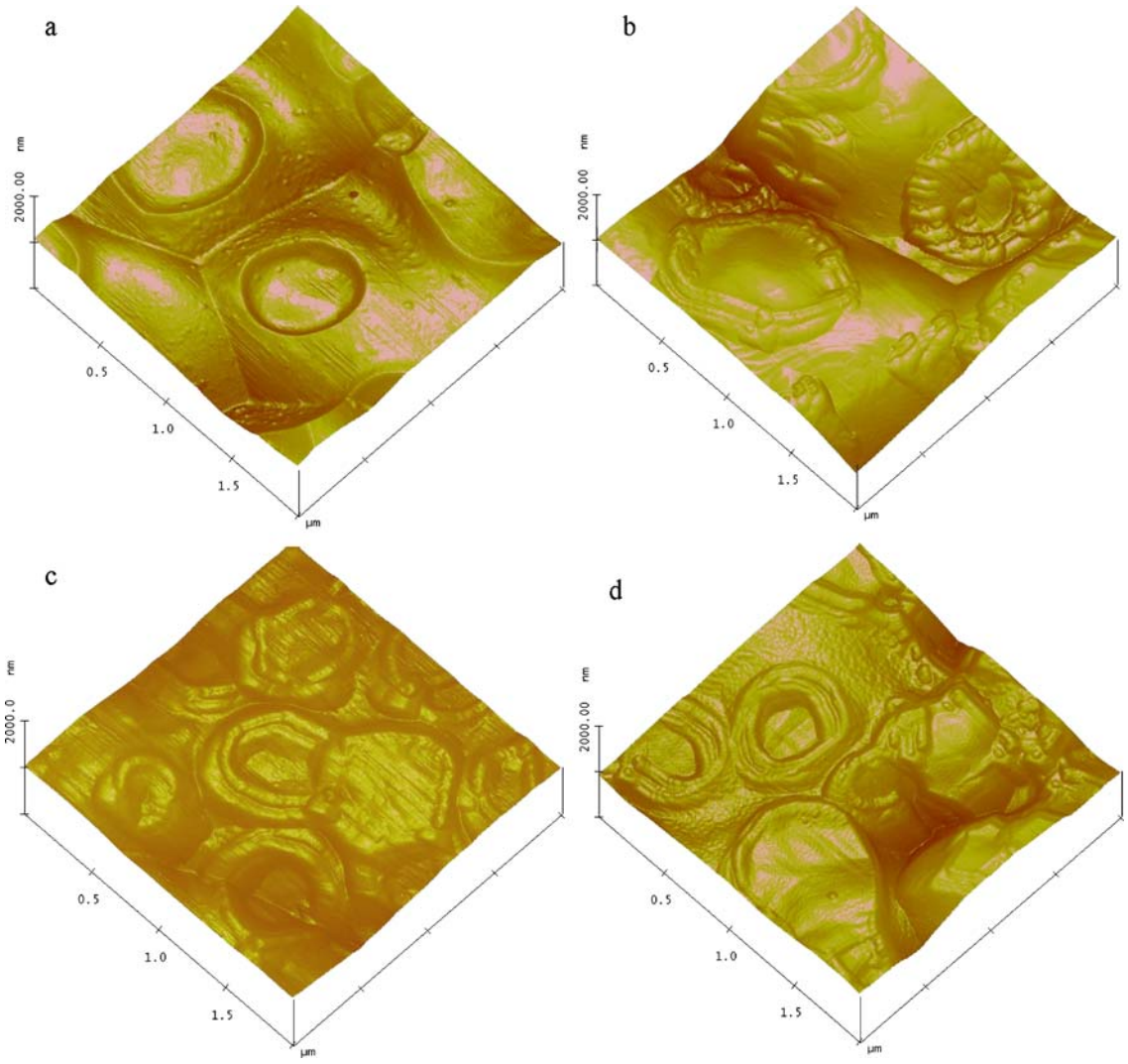

Fig. 7 AFM images of the YSZ electrolyte surface in contact with the LSM electrode **a** before the polarization and **b** after cathodic current passage for 3 h, **c** cathodic and anodic current passage for 6 h, and **d** anodic current passage for 3 h. All polarization treatments were performed under a current of 200 mA cm^{-2} at 800°C in air. The LSM electrode was removed by HCl treatment [24]

rings, indicating that there is no formation of a secondary phase such as lanthanum zirconate between A-site deficient LSM and YSZ under the experimental conditions in this study [25]. After the polarization treatments, the sharp edge of the YSZ rings disappeared and the rings grew outwards. Despite the difference in the polarization treatment programs, the changes in the morphology and topography of the convex rings are similar. The circumference of the rings grew to a two-dimensional boundary area. The width of the rings is in the range 0.08 to 0.23 µm, and the average ring width is 0.15±0.05 µm. It is noted that such interfacial changes induced by the cathodic polarization are not reversible under subsequent anodic polarization (Fig. 7c). Moreover, the anodic current treatment on a freshly prepared LSM electrode also induced a change in LSM/YSZ interface topography similar to the cathodic current treatment (Fig. 7d). This indicates that the initial LSM/YSZ interface formed by the thermal treatment of the system is morphologically unstable. Both cathodic and anodic current passage has a significant effect on the morphology and topography of the LSM electrode/YSZ electrolyte interface. The formation of a convex ring on the YSZ electrolyte surface and its subsequent broadening under various polarization treatments indicate that oxygen reduction and oxidation reactions most likely occur at the O_2/LSM/YSZ three phase boundary areas.

Effect of surface species and relaxation of the activation of the LSM cathode

The most direct evidence of the significant dependence of the surface species/composition of the LSM electrodes on the activation process was provided by the activation behavior on a weakly acid-etched freshly prepared LSM electrode [16]. In this experiment, an as-prepared $La_{0.72}Sr_{0.18}MnO_3$ electrode was treated with 1 M HCl acid solution prior to the cathodic polarization. Figure 8 shows the initial

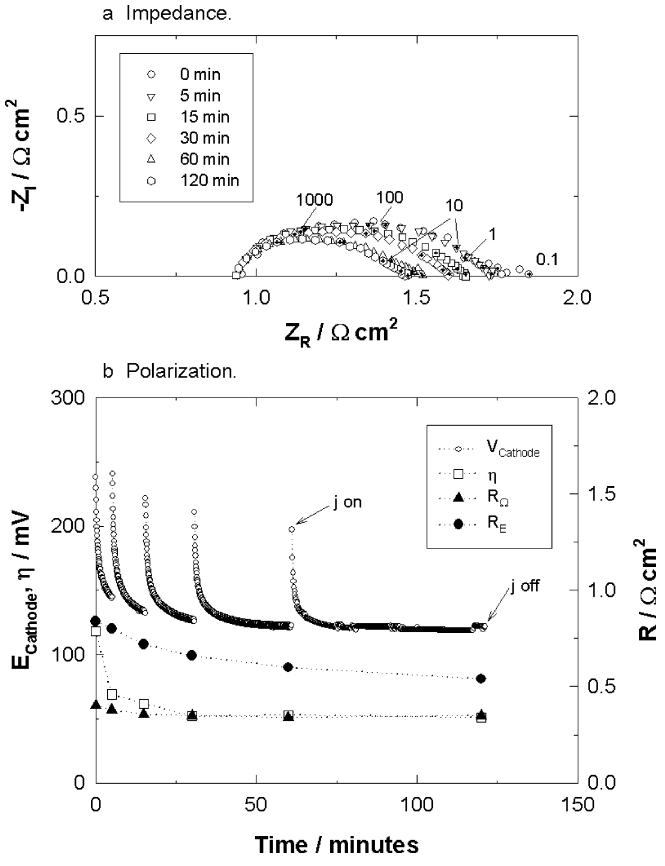

Fig. 8 Initial impedance curves of the 1-M HCl acid-etched LSM under a cathodic current of 200 mA cm^{-2} at 900°C in air [16]. The *numbers* are the frequencies in hertz

impedance curves of the acid-etched LSM under a cathodic current of 200 mA cm^{-2} at 900°C in air. Compared to the LSM electrode with the same composition but without acid etching (Fig. 1), the initial electrode polarization behavior of the acid-etched LSM is distinctively different. First, the initial electrode polarization resistance R_E is significantly smaller. The R_E for the reaction on acid-etched LSM is 0.84 Ω cm^2, much smaller than the reaction on LSM without acid etching (6.2 Ω cm^2). Second, the reduction in R_E under the cathodic polarization treatment is also much smaller. After the cathodic current passage for 15 min, the R_E value is 0.73 Ω cm^2. This is close to the initial value of 0.84 Ω cm^2 before the current treatment. In contrast, for the reaction on LSM without acid etching, R_E is reduced from 6.2 to 0.7 Ω cm^2 after the cathodic current passage for 15 min (Fig. 1a). This demonstrates that the activation process for the O_2 reduction on acid-etched LSM is not as effective as the activation without acid-etching treatment.

The inductively coupled plasma atomic emission spectroscopy (ICP-AES) analysis of the solution collected after the HCl etching of the LSM electrode coating shows that the concentration of Sr and Mn is one order of magnitude higher than that of La [16]. The atomic ratio of the La/Sr/Mn based on the La concentration is 0.74/8.4/15.8 for the etched solution, significantly differently from the measured ratio of 0.74/0.15/1 for the LSM coating. The high content of Mn may not be surprising as the measured LSM is A-site substoichiometry with small Mn excess. However, the high content of Sr on the LSM surface is an indication of the Sr enrichment on the LSM surface, consistent with the surface analysis of the high Sr and oxygen content on the surface of fine LSM grains [26]. This indicates that the surface composition of LSM is not the same as that of the bulk and that SrO is most likely enriched or segregated on the surface of the as-prepared LSM electrodes.

The relaxation of the electrode polarization resistance after the interruption of the cathodic polarization/current treatment is another interesting phenomenon associated with the activation. After interruption of the polarization, the potential of the cathode returns to zero almost instantaneously. However, the electrode impedance evolves slowly to the original [1, 14, 27]. The high-frequency impedance remains more or less constant, and the significant change in the electrode impedance is mainly in the low-frequency range [27]. Figure 9 shows the relaxation of the electrode polarization resistance measured on an LSM electrode under open circuit after it was polarized at a cathodic current passage of 200 mA cm^{-2} for 3 h at 700°C. The inset graph is the plot of R_E vs $t^{1/2}$. After evolving for 67 h at open circuit, the electrode polarization resistance is 109 Ω cm^2, close to 118 Ω cm^2 for the reaction on the freshly prepared LSM before the activation process. If the relaxation process is only limited by the oxygen ion diffusion, the relaxation time of the electrode performance would be in the order of minutes rather than hours based on the relatively fast oxygen ion diffusion [28]. The very slow relaxation process may indicate the involvement of the cation diffusion as the cation diffusion in perovskite-based oxides is at least three to four orders of magnitude lower than that of oxygen vacancies at the same temperature [29, 30]. The two different slopes in the relaxation curves indicate that the electrode relaxation might be limited by two elementary steps.

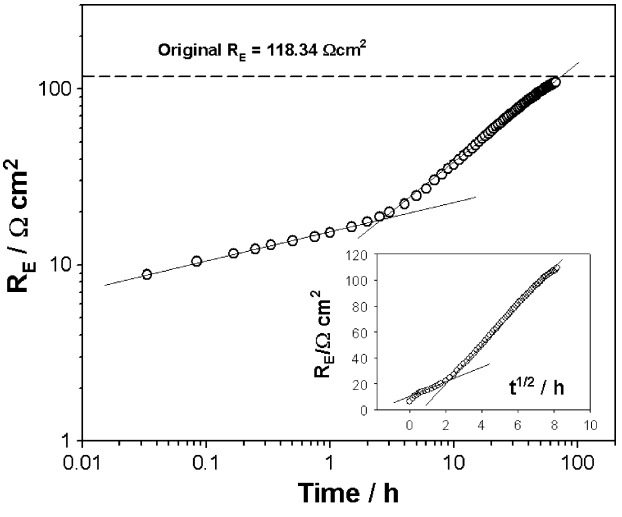

Fig. 9 Relaxation of electrode polarization resistance measured on LSM electrodes after the cathodic current passage at 200 mA cm^{-2} for 3 h at 700°C. The *inset graph* is the plot of R_E vs $t^{1/2}$

Mechanism of the activation process

The activation process has been studied generally as part of the mechanism and kinetic studies of the oxygen reduction reaction. The conventional explanation for the activation process on LSM-based electrodes is based on the formation of oxygen vacancies in the LSM under cathodic polarization [11–15]. Under fuel cell operating conditions, oxygen vacancies are generated at the electrode/electrolyte interface region with a charge compensation by the reduction in B-site transition metal ions (eg., Mn^{3+} to Mn^{2+}) according to [13]:

$$O^{x}_{O,LSM} + 2Mn^{\bullet}_{Mn,LSM} + V^{\bullet\bullet}_{O,YSZ} + 2e' \rightarrow +V^{\bullet\bullet}_{O,LSM} + 2Mn^{x}_{Mn,LSM} + O^{X}_{O,YSZ} \quad (1)$$

$$O^{x}_{O,LSM} + 2Mn^{x}_{Mn,LSM} + V^{\bullet\bullet}_{O,YSZ} + 2e' \rightarrow V^{\bullet\bullet}_{O,LSM} + 2Mn'_{Mn,LSM} + O^{X}_{O,YSZ} \quad (2)$$

where $Mn^{\bullet}_{Mn,LSM}$, $Mn^{x}_{Mn,LSM}$ and $Mn'_{Mn,LSM}$ donate Mn^{4+}, Mn^{3+} and Mn^{2+} ions on LSM lattice sites, respectively, and $O^{x}_{O,YSZ}$ and $V^{\bullet\bullet}_{O,YSZ}$ are the O^{2-} ions and oxygen vacancies on YSZ lattice sites, respectively. Oxygen vacancies formed at the LSM/YSZ interface region would propagate, extending the reactive sites for the O_2 reduction reaction. The improvement in electrochemical activity results from the broadening of the active reaction zone [11–15]. The deactivation effect of the reaction under anodic polarization/current passage is explained by the partial oxidation of the Mn ions and the elimination of oxygen vacancies, i.e., the reverse process of reactions (1) and (2) [3]. The low electrochemical activity of the LSM cathode is due to the observed very low oxygen ion conductivity of the LSM materials [31, 32]. Considering that the dominant defects in the LSM under open circuit are cation vacancies, Chen et al. [33] modified the oxygen vacancy formation mechanism and suggested that the reduction in manganese at the initial stage of cathodic polarization ions occurs with the concomitant removal of cation vacancies on A and B sites:

$$V'''_{La,LSM} + V'''_{Mn,LSM} + 3O^{x}_{O,LSM} + 6Mn^{\bullet}_{Mn,LSM} + 3V^{\bullet\bullet}_{O,YSZ} + 6e' \rightarrow 6Mn^{x}_{Mn,LSM} + 3O^{x}_{O,YSZ} \quad (3)$$

where $V'''_{La,LSM}$ and $V'''_{Mn,LSM}$ are cation vacancies on LSM lattice sites.

However, the mechanism based on the removal of cation vacancies and/or the formation of oxygen vacancies under cathodic polarization and the elimination of the oxygen vacancies under anodic polarization is not adequate to explain the observed activation and deactivation behavior under the cathodic and anodic polarization/current passage. If the significant reduction in the electrode polarization resistance, as observed on the as-prepared LSM (see Fig. 1), is purely due to the formation of oxygen vacancies or the removal of cation vacancies, such an activation process should not be greatly affected by the surface acid treatment of LSM because the formation of oxygen vacancies is a process induced by the cathodic polarization. In addition, as shown in Fig. 3, the activation process under cathodic polarization and the deactivation process under anodic polarization for the reaction on LSM electrodes is not reversible. The deactivation under anodic polarization is a relatively slow process in comparison with that of the activation under cathodic polarization. The observed very slow relaxation process of the electrode process after the interruption of the cathodic polarization is also not consistent with the relatively fast anion diffusion process. Thus, the defect model as illustrated in Eqs. 1, 2, and 3 cannot explain the observed activation effect of cathodic polarization/current treatment.

To understand the origin of the activation process, we need to examine the issue of the Sr enrichment/segregation on the LSM surface. The elemental analysis of the acid etching of the LSM electrode coating indicates that SrO might be enriched at the surface of the LSM grains. The SrO enrichment on the surface of LSM grains is also indicated by X-ray photoelectron spectroscopy (XPS) studies, although the XPS averages over about 10 atomic monolayers. The most direct evidence of the Sr segregation is probably the one provided by Majkic et al. on the study of the stress-induced diffusion and defect chemistry of $La_{0.2}Sr_{0.8}Fe_{0.8}Cr_{0.2}O_{3-\delta}$ (LSFCr) [34]. When the specimen was quenched from 1,100°C, the Sr-3d region on the XPS spectra shifted to higher binding energies for samples that were quenched in oxygen partial pressure (10^{-10}–10^{-13}) in comparison to the sample quenched in air. This indicates more surface-bounded Sr on the samples quenched from low oxygen partial pressure. On a creep-quenched LSFCr specimen, the elemental map of ^{88}Sr by the secondary ion mass spectroscopy (SIMS) technique revealed the Sr segregation at grain boundaries, and the corresponding elemental maps of La, Fe, and Cr revealed no grain boundary segregation. Detailed XPS study of $La_{1-x}Sr_x$-based perovskite-type oxides including $La_{0.4}Sr_{0.6}Fe_{0.8}Co_{0.2}O_3$ also revealed the strontium segregation towards the surface [35]. Viitanen et al. [36] studied the surface compositions of $La_{0.6}Sr_{0.4}Co_{0.2}Fe_{0.8}O_3$ (LSCF) oxide membranes by low-energy ion spectroscopy (LEIS). Before the oxygen permeation experiments, the LEIS measurements only showed the presence of La, Sr, and O in the outermost atomic layer and no Fe and Co on the contamination-free LSCF membranes. This suggests that Sr species are originally enriched or segregated at the surface of LSCF and, probably to a lower degree, at the surface of LSM. This may stem from the abrupt termination of the lattice structure, which decreases the stability and induces segregation and structural distortion over the outermost atomic layer. Since Sr does not exist in the free state, the Sr-enriched regions are most likely in the form of SrO. The observation of the remarkable effect of the weak acid etching on the ac-

tivation behavior of the LSM electrode (Fig. 8) indicates that there is a mechanism to remove passive SrO species on the LSM surface under cathodic polarization/current treatment.

Partial doping of the La^{3+} site in $LaMnO_3$ perovskites with low-valent cations (eg., Sr^{2+}) leads to an increase in the valence of the B-site Mn metal ions (as positive holes) and/or the formation of oxygen vacancies. The dominant defect is largely a function of the partial pressure of oxygen and can display both oxygen-excess and oxygen-deficient stoichiometry, as shown by numerous thermodynamic defect models [37–39]. Oxygen vacancies become dominant only at much lower oxygen partial pressures ($<< 10^{-5}$ Pa) [38]. Under relatively high oxygen partial pressures and open circuit, LSM becomes oxygen-excess. Since the close-packed ABO_3 perovskite structure cannot accommodate an excess of oxygen as an interstitial oxygen ion due to its large radius, cation vacancies would be the dominant defect according to [38]:

$$nil \Leftrightarrow V'''_{La} + V'''_{Mn} + 3V^{\bullet\bullet}_{O,LSM} \tag{4}$$

The existence of cation vacancies has been confirmed by neutron powder diffraction studies [40–42]. As shown by Mitchell et al. [40], cation vacancies in LSM most likely occur on the A-site (e.g., the La/Sr site), rather than on the B-site (e.g., the Mn site).

For the O_2 reduction reaction on the as-prepared LSM electrodes, the SrO originally enriched or segregated on the LSM surface could occupy the active sites and inhibit the surface dissociation and diffusion process. This would lead to the initially very high R_E and overpotential (Fig. 1). Thus, removal of the SrO species by a chemical process such as weak acid etching can lead to the significant improvement of the initial polarization performance and to the significant reduced activation effect of the cathodic polarization treatment (Fig. 8). Similarly, the significant reduction in the electrode interface resistance and polarization potential after the application of a cathodic polarization/current passage at SOFC operating temperatures provides a strong evidence of the incorporation of the segregated SrO species into the LSM perovskite lattice with the concomitant removal of the cation vacancies. Cook et al. [43] studied the deformation and creep behavior of LSM as a function of oxygen partial pressure and Sr content. His study concluded that the dependence of the steady-state stress and strain rate on the oxygen partial pressure and Sr-content could be explained using a modified defect model that involves the incorporation of SrO and Mn_2O_3 species into the lattice of $LaMnO_3$:

$$2SrO + Mn_2O_3 \rightarrow 2Sr'_{La,LSM} + 5O^x_{O,LSM} + 2Mn^x_{Mn,LSM} + V^{\bullet\bullet}_{O,LSM} \tag{5}$$

$$2SrO + Mn_2O_3 + \frac{1}{2}O_2 \rightarrow 2Sr'_{La,LSM} + 6O^x_{O,LSM} + 2Mn^x_{Mn,LSM} \tag{6}$$

where $Sr'_{La,LSM}$ represents an Sr ion incorporated into the La site in LSM lattice. The incorporation/segregation of constituent elements in perovskite oxides under reducing/oxidizing environment was also reported on a $Ba_{0.5}Sr_{0.5}Co_{0.8}Fe_{0.2}O_3$ ceramic membrane reactor for methane oxidation [44]. Co and Fe species originated during the reduction were found to be incorporated into the perovskite structure after the subsequent oxidation treatment.

Thus, considering the predominant A-site cation vacancies and the segregated SrO on the LSM electrode surface under open circuit conditions, the initial significant reduction in the electrode interface resistance and overpotential for the O_2 reduction reaction on as-prepared LSM electrode is most likely due to the incorporation of passive species such as SrO into the LSM perovskite structure under the cathodic polarization/current passage treatment:

$$2SrO \rightarrow 2Sr'_{La,LSM} + 2O^x_{O,LSM} + V^{\bullet\bullet}_{O,LSM} \tag{7}$$

The incorporation of SrO would be kinetically favorable due to the existence of the cation vacancies at the A-site. With the removal of SrO species on the LSM surface, the reduction in manganese ions will occur with the concomitant formation of oxygen vacancies (Eqs. 1 and 2) under continuing cathodic polarization conditions [13]. This indicates that the activation of the O_2 reduction reaction on LSM electrodes would be limited by two processes: the removal of SrO species and the formation of oxygen vacancies. The first step is responsible for the initial rapid improvement of the electrocatalytic activity of the LSM electrode under the cathodic polarization.

Under anodic polarization, the oxygen vacancies are consumed by the recombination reactions (the reverse reaction of Eqs. 1 and 2), followed by the cation vacancy formation. As the cation vacancy formation would result in the segregation of Sr on the LSM surface, the process would be highly energetic and would be much slower as compared to the corresponding Sr incorporation process. This explains the much slower deactivation rate for the reaction on the LSM electrode under anodic polarization in comparison with the activation rate for the reaction on the LSM electrode under cathodic polarization (Fig. 3).

After the interruption of the cathodic polarization, the relaxation of the electrode polarization behavior under open circuit is also governed by two steps: the disappearance of oxygen vacancies and the formation of cation vacancies with the concomitant segregation of SrO, similar to that under anodic polarization. The consumption of oxygen vacancies due to the recombination could be an instantaneous process. However, the formation of cation vacancies with the concomitant segregation of Sr could be much slower without the external anodic polarization driving force. The cation diffusion coefficient in the perovskite structure is at least three to four orders of magnitude lower than that of oxygen at the same temperature and oxygen partial pressure [30, 31, 33, 45]. For the perovskite-based oxides, the activation energy of the cation vacancy diffusion is also much higher than that of oxygen vacancy diffusion [46, 47]. Thus,

due to the limited cation diffusion process, the formation of the cation vacancies would be kinetically unfavorable and slow in comparison with the consumption of the oxygen vacancy. The slow and dominant cation vacancy formation with the concomitant segregation of SrO explains the observed slow relaxation process of the electrode polarization resistance as shown in Fig. 9. The appearance of two slopes in the relaxation curve could be an indication of the two limiting processes as discussed above.

Conclusions

Polarization treatments not only have a significant effect on the electrochemical activity for the oxygen reduction reactions of the LSM electrodes, but also have a significant effect on the microstructure and morphology of the LSM electrode itself and on the LSM electrode/YSZ electrolyte interface. Under cathodic polarization, both the generation and migration of oxygen vacancies and Mn ions, the lattice expansion, and the crystallographic distortion can all contribute to the microstructural changes. Similar to the observations made under cathodic current passage, the anodic current passage also induces microstructure and morphology improvement on the freshly prepared LSM electrode, which is most likely due to the lattice shrinkage in the oxidizing environment.

The mechanism of activation process for the O_2 reduction on LSM electrode can be explained by the removal of SrO species on the LSM surface followed by the reduction in manganese ions with the concomitant formation of oxygen vacancies. The deactivation process for the reaction on LSM electrodes under anodic polarization or under open circuit conditions is basically the reverse of the activation process: the consumption of oxygen vacancies and the formation of cation vacancies with the concomitant segregation of SrO species on the LSM surface. However, due to the very slow kinetics of the cation diffusion process, the formation of cation vacancies with the segregation of SrO species is a slow step, particularly under open circuit, in comparison with the disappearance of the oxygen vacancies.

References

1. van Heuveln FH, Bouwmeester HJM (1997) J Electrochem Soc 144:134
2. Jiang SP, Love JG, Zhang JP, Hoang M, Ramprakash Y, Hughes AE, Badwal SPS (1999) Solid State Ionics 121:1
3. Chen XJ, Khor KA, Chan SH (2004) Solid State Ionics 167:379
4. McIntosh S, Adler SB, Vohs JM, Gorte RJ (2004) Electrochem Solid-State Lett 7:A111
5. Kim J-D, Kim G-D, Moon J-W, Park Y-I, Lee W-H, Kobayashi K, Nagai M, Kim C-E (2001) Solid State Ionics 143:379
6. Leng YJ, Chan SH, Khor KA, Jiang SP (2004) J Appl Electrochem 34:409
7. Sridhar S, Stancovski V, Pal UB (1997) Solid State Ionics 100:17
8. Jacobsen T, Zachau-Christiansen B, Bay L, Jørgensen MJ (2001) Electrochim Acta 46:1019
9. McEvoy AJ (2003) Solid State Ionics 135:331
10. Zachau-Christiansen B, Jacobsen T, Bay L, Skaarup S (1998) Solid State Ionics 113–115:271
11. Hammouche A, Siebert E, Hammou A, Kleitz M, Caneiro A (1991) J Electrochem Soc 138:1212
12. Jiang Y, Wang S, Zhang Y, Yan J, Li W (1998) J Electrochem Soc 145:373
13. Lee HY, Cho WS, Oh SM, Wiemhöfer H-D, Göpel W (1995) J Electrochem Soc 142:2659
14. Odgaard M, Skou E (1996) Solid State Ionics 86–88:1217
15. Siebert E, Hammouche A, Kleitz M (1995) Electrochim Acta 40:1741
16. Jiang SP, Love JG (2001) Solid State Ionics 138:183
17. Jiang SP (2003) J Power Sources 124:390
18. Lee Y-K, Kim J-Y, Lee Y-K, Kim I, Moon H-S, Park J-W, Jacobson CP, Visco SJ (2003) J Power Sources 115:219
19. Wang W, Jiang SP (2004) J Solid State Electrochem 8:914
20. Tsukuda H, Yamashita A (1994) In: Bossel U (ed) Proceedings of the 1st European SOFC forum. European Fuel Cells Group, Lucerne, Switzerland, p 715
21. Kuznecov M, Otschik P, Obenaus P, Eichler K, Schaffrath W (2003) Solid State Ionics 157:371
22. Jiang SP, Love JG (2003) Solid State Ionics 158:45
23. Jiang SP, Wang W (2005) Solid State Ionics 176:1185
24. Jiang SP, Wang W (2005) Electrochem Solid-State Lett 8:A115
25. Mitterdorfer A, Gauckler LJ (1998) Solid State Ionics 111:185
26. Decorse P, Caboche G, Dufour L-C (1999) Solid State Ionics 117:161
27. Gharbage B, Pagnier T, Hammou A (1994) J Electrochem Soc 141:2118
28. Adler SB (2004) Chem Rev 104:4791
29. Kawada T, Horita T, Sakai N, Yokokawa H, Dokiya M (1995) Solid State Ionics 79:201
30. Horita T, Ishikawa M, Yamaji K, Sakai N, Yokokawa H, Dokiya M (1998) Solid State Ionics 108:383
31. Yasuda I, Ogasagawa K, Hishinuma M, Kawada T, Dokiya M (1996) Solid State Ionics 86–88:1997
32. Carter S, Selcuk A, Chater RJ, Kajda J, Kilner JA, Steele BCH (1992) Solid State Ionics 53–56:597
33. Chen XJ, Chan SH, Khor KA (2004) Electrochem Solid State Lett 7:A144
34. Majkic G, Mironova M, Wheeler LT, Salama K (2004) Solid State Ionics 167:243
35. van der Heide PAW (2002) Surf Interface Anal 33:414
36. Viitanen MM, Welzenis RGV, Brongersma HH, van Berkel FPF (2002) Solid State Ionics 150:223
37. Mizusaki J, Mori N, Takai H, Yonemura Y, Minamiue H, Tagawa H, Dokiya M, Inaba H, Naraya K, Sasamoto T, Hashimoto T (2000) Solid State Ionics 129:163
38. Nowotny J, Rekas M (1998) J Am Ceram Soc 81:67
39. Poulsen FW (2000) Solid State Ionics 129:145
40. Mitchell JF, Argyriou DN, Potter CD, Hinks DG, Jorgense JD, Bader SD (1996) Phys Rev B 54:6172
41. van Roosmalen JAM, Cordfunke EHP, Helmhodt RB, Zandberg HW (1994) J Solid State Chem 110:100
42. Alonso JA, Martinez-Lope MJ, Casais MT, MacManus-Driscoll JL, de Silva PSIPN, Cohen LF, Fernández-Diaz MT (1997) J Mater Chem 7:2139
43. Cook RE, Goretta KC, Wolfenstine J, Nash P, Routbort JL (1999) Acta Mater 47:2969
44. Shao ZP, Dong H, Xiong GX, Cong Y, Yang WS (2001) J Membr Sci 183:181
45. Schulz O, Martin M (2000) Solid State Ionics 135:549
46. de Souza RA, Islam MS, Ivers-Tiffée E (1999) J Mater Chem 9:1621
47. Cherry M, Islam MS, Catlow CRA (1995) J Solid State Chem 118:125